Adv Biochem Engin/Biotechnol (2011) 124: 1–19
DOI: 10.1007/10_2010_81

Published Online: 12 November 2010

Light Microscopic Analysis of Mitochondrial Heterogeneity in Cell Populations and Within Single Cells

Stefan Jakobs, Stefan Stoldt and Daniel Neumann

Abstract Heterogeneity in the shapes of individual multicellular organisms is a daily experience. Likewise, even a quick glance through the ocular of a light microscope reveals the morphological heterogeneities in genetically identical cultured cells, whereas heterogeneities on the level of the organelles are much less obvious. This short review focuses on intracellular heterogeneities at the example of the mitochondria and their analysis by fluorescence microscopy. The overall mitochondrial shape as well as mitochondrial dynamics can be studied by classical (fluorescence) light microscopy. However, with an organelle diameter generally close to the resolution limit of light, the heterogeneities within mitochondria cannot be resolved with conventional light microscopy. Therefore, we briefly discuss here the potential of subdiffraction light microscopy (nanoscopy) to study inner-mitochondrial heterogeneities.

Keywords Fluorescence microscopy · Mitochondria · Nanoscopy · Single-cell heterogeneity · Super-resolution microscopy

Abbreviations

GSD microscopy	Ground state depletion microscopy
GSDIM	Ground state depletion microscopy followed by individual molecule return
MMP	Mitochondrial membrane potential
PALM	Photoactivated localization microscopy
RESOLFT	Reversible saturable/switchable optical linear (fluorescence) transitions
STED microscopy	Stimulated emission depletion microscopy
STORM	Stochastic optical reconstruction microscopy
TOM	Translocase of the outer membrane

S. Jakobs (✉), S. Stoldt and D. Neumann
Mitochondrial Structure and Dynamics Group,
Max Planck Institute for Biophysical Chemistry, Am Fassberg 11,
37077 Goettingen, Germany
e-mail: sjakobs@gwdg.de

Contents

1 Mitochondria: The Powerhouses of the Cell

Oxidative phosphorylation (OXPHOS) takes place in mitochondria, and thus these organelles are crucial for the regeneration of ATP from ADP and inorganic phosphate in respiration [112]. They are the 'powerhouses of the cell' [84, 115]. In addition, several other essential metabolic pathways take place in these organelles, such as the β-oxidation of fatty acids [66], the formation of iron-sulfur centers [76], the urea cycle, as well as the biogenesis of pyridines, nucleotides and phospholipids [116]. Mitochondria take part in the cellular Ca^{2+} homeostasis [61, 127], and they play an important role during the progression of programmed cell death referred to as apoptosis [25, 42, 70].

Especially in the last 2 decades, it has become clear that mitochondria also play a crucial role in a number of human diseases [36, 94], including diabetes mellitus [93], cancer [12, 15, 86], neurodegenerative diseases such as Parkinson's and Alzheimer's [72, 106, 128], and several others. Further, mitochondrial (dis-) function has been linked to the cellular aging processes, characterized by impaired levels of oxidative phosphorylation and increasing amounts of reactive oxygen species [88, 115].

2 Mitochondrial Heterogeneity Between Different Species

The term mitochondrium [6] is derived from the Greek words *mitos*, which stands for fiber or thread, and *chondros*, which means grain or corn. Put together, they can be translated as a thread-like grain; thus, the word already indicates the heterogeneity of the mitochondrial morphology, which has been known since this organelle was first described [68].

In the last 3 decades, most studies investigating the morphology and dynamics of mitochondria have relied on various forms of far-field fluorescence microscopy imaging mitochondria that were stained with specific fluorescent dyes or tagged with fluorescent proteins [62]. Mitochondrial morphology and dynamics have been studied in many eukaryotic organisms, ranging from monocellular yeasts [63, 95, 96] to higher multicellular eukaryotes, including plants [3, 77, 122] and mammals [7, 27, 71, 75, 108].

Examples of diverse mitochondrial shapes in different organisms are shown in Fig. 1. The spherical mitochondria in the guard cells of a tobacco plant (Fig. 1b) vary considerably from the tubular mitochondria in budding yeast (Fig. 1a) or from the complex mitochondrial networks of a cultivated human cancer cell (Fig. 1c). Mitochondria in plant cells often do not form a continuous network, and they are frequently located next to chloroplasts. Indeed, plant mitochondria differ substantially from mitochondria of other eukaryotes in a number of aspects, including different strategies for genome maintenance, genetic decoding, gene regulation and organelle segregation [9, 80, 104, 105]. In the plant Arabidopsis thaliana, the mitochondrial proteome encompasses about 3,000 proteins [10], whereas about 1,000 different mitochondrial proteins were predicted for budding yeast [85, 103] and about 1,500 for human cells [85].

3 Mitochondrial Heterogeneity Between Different Cell Types

In most cultivated mammalian cells mitochondria form a complex, more or less connected network [39]. These mitochondria have a similar set of proteins and fulfill similar metabolic needs; still, their actual shape may vary considerably:

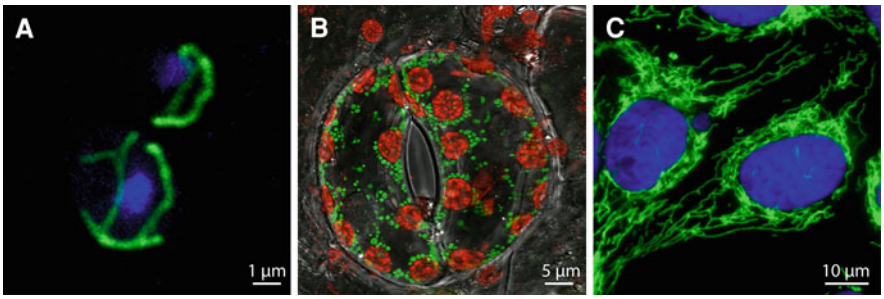

Fig. 1 Different mitochondrial morphologies in fungi, plant and mammalian cells. Fluorescence micrographs of the budding yeast *Saccharomyces cerevisiae* (**a**), a guard cell of the tobacco plant *Nicotiana tabacum* (**b**) and a cultured human (U2OS) cell (**c**). In **a** and **b** the mitochondria (*green*) were labeled by the expression of the green fluorescent protein (GFP) targeted to the mitochondrial matrix. In **c** the mitochondria (*green*) were immunostained by an antibody against the mitochondrial outer membrane protein Tom20. The chloroplasts (**b**) (*red*) were visualized using their strong autofluorescence. The nuclei (**a**, **c**) (*blue*) were highlighted with DAPI

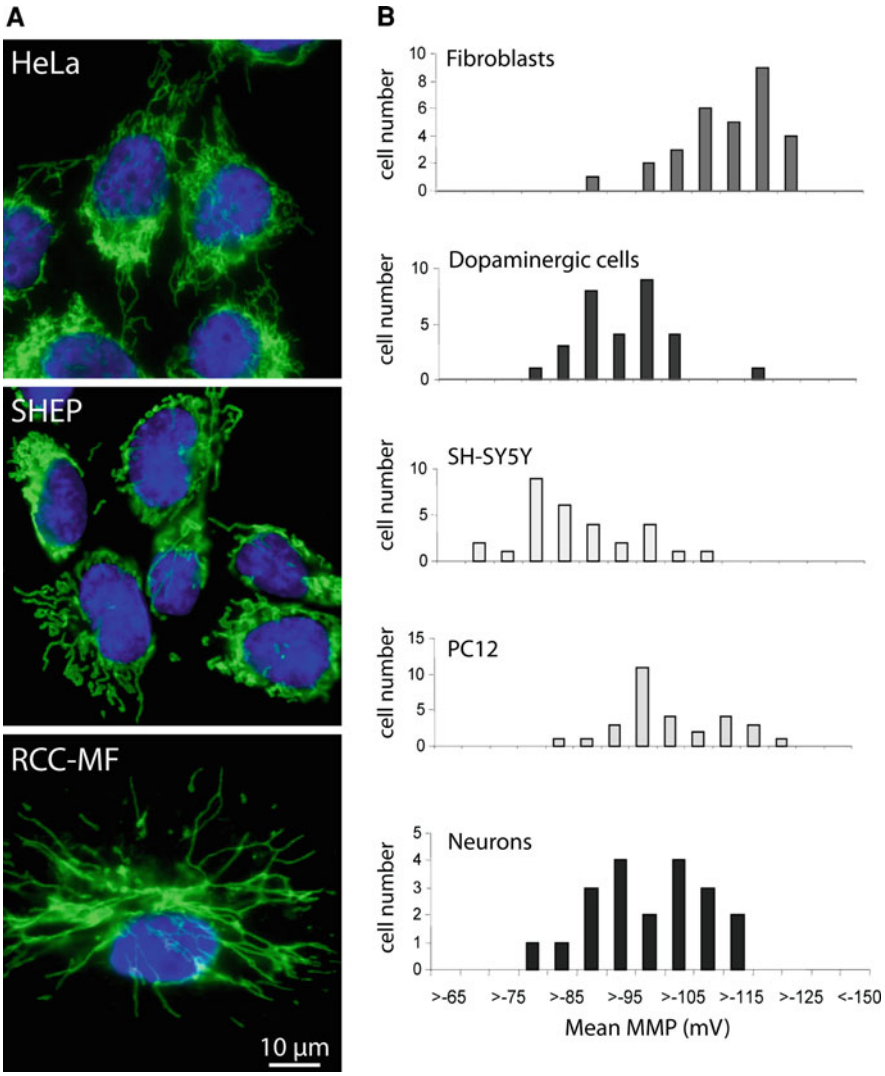

Fig. 2 Mitochondrial heterogeneities between different mammalian cell types. **a** The overall mitochondrial morphologies differ between three human carcinoma cell types (HeLa cervical carcinoma, SHEP neuroblastoma, RCC-MF renal cell carinoma). Mitochondria were immunostained with an antiserum against the mitochondrial protein Tom20; the nuclei were labeled with DAPI. Shown are representative images taken with an epi-fluorescence microscope. **b** The mitochondrial membrane potential (MMP) reflects the functional status of mitochondria. The mean MMP varies significantly between different mammalian cell types (from [58], with permission)

Whereas the mitochondria of HeLa (derived from a human cervical carcinoma) and SHEP (derived from a human neuroblastoma) cells build up a highly interconnected, dense meshwork of slightly curled mitochondrial tubules; the mitochondria of RCC-MF (human renal cell carcinoma) cells are much less interconnected, and the straight mitochondrial tubules appear to radiate from the nucleus (Fig. 2a). However, a more spherical grain-like morphology has been observed in a few cell types [2, 20]. Moreover, in addition to these overall shape differences, also more subtle but characteristic distinctions in the diameter of the mitochondrial tubules of different cell types have been reported [31].

Morphologic shape differences in genetically similar cells are not restricted to closely related mammalian cell lines, but have also been described in other kingdoms. For example, in most plant tissues, the mitochondria exhibit spherical structures of uniform diameter. However, in certain cell types within the vascular tissue, the shapes range from sausage-shaped to long worm-like forms [78].

In addition to these morphological variations, Huang et al. reported on different mitochondrial membrane potentials in various mammalian cell types (Fig. 2b). The mitochondrial membrane potential is a key indicator of cellular viability, as it reflects the pumping of protons across the inner membrane during the process of electron transport and oxidative phosphorylation. The mean MMP in the analyzed cell types ranged from -112 ± 2 mV in fibroblasts to -87 ± 2 mV in SH-SY5Y cells, suggesting specific adaptations to the energy demands of the respective cells [58].

Hence, there can be large differences in the shapes of the mitochondria of different cells. Some of these differences may be attributed to different functional tasks of the respective cells, whereas other shapes are less obvious to comprehend. Obviously, cells have a wide repertoire of potential mitochondrial morphologies that may be adapted to the specific metabolic state of the cell.

4 Mitochondrial Shape Changes in a Cell Over Time

4.1 Structural Adaptations to the Cellular Energy Demands

The main physiological role of mitochondria is to generate ATP. Frequently, a connection between mitochondrial structure and the bioenergetical requirements of the cell has been suggested [5, 13, 109, 131]. For example, in budding yeast cells (*S. cerevisiae*), the volume of the mitochondrial reticulum is increased up to three-fold after changing from a fermentable (glucose) to a non-fermentable (glycerol) carbon source (Fig. 3a) [34, 125]. When glucose is available in large amounts in the budding yeast, respiration is repressed and ATP is primarily produced via glycolysis (without involvement of mitochondria), a phenomenon also known as the “Crabtree effect” [24, 26, 29, 37]. Therefore, only under non-fermentable

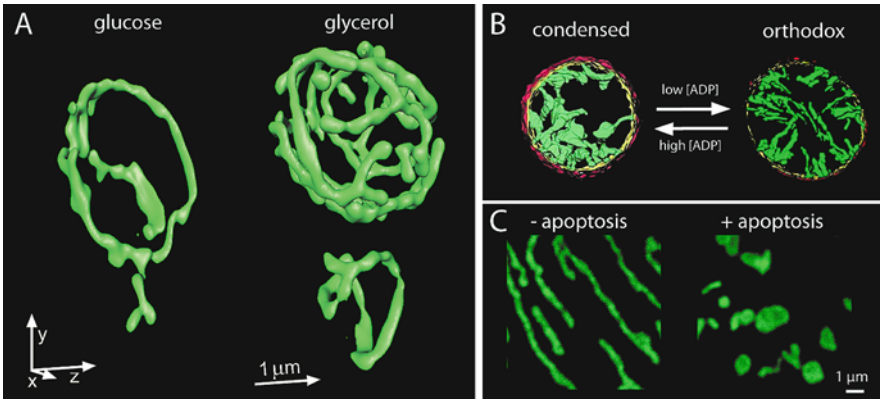

Fig. 3 Mitochondrial shape adaptations to different conditions. **a** The mitochondrial network of the budding yeast *S. cerevisiae* adapts to different carbon sources in the growth medium. Shown are 3D reconstructions of the mitochondria of living cells labeled with the green fluorescent protein (GFP). The cells were grown in a fermentable (glucose) or a non-fermentable (glycerol) growth medium. Images were taken with a multifocal multiphoton 4Pi-confocal microscope (from [34], with permission). **b** Electron tomographic reconstructions of rat liver mitochondria reveal changes in the mitochondrial inner membrane topology associated with the orthodox-condensed transition. The mitochondrial outer membrane is shown in *red*, the inner boundary membrane in *yellow* and the cristae in *green*. The depicted mitochondria have diameters of 1,500 nm (*left*) and 500 nm (*right*) (from [82], with permission). **c** Mitochondria in unchallenged cultivated mammalian cells (U2OS) adopt a tubular shape, forming an interconnected network (*left*). Upon induction of apoptosis (10 µM actinomycin D for 12 h), the network fragments, resulting in numerous small mitochondria with a spherical shape (*right*). For visualization, the mitochondria were labeled with an antiserum against the mitochondrial protein Tom20 and imaged with a confocal microscope

conditions are mitochondria required for ATP production. This is a clear example of mitochondrial shape adaptations to different energy needs.

Likewise, it has been reported that in drought-stressed spinach leaves, a decrease of the mitochondrial volume in parenchyma cells can be observed [138]. This reduced mitochondrial volume has been suggested to be caused by glucose starvation deriving from decreased photosynthetic activity.

The energy requirements of the cell may also influence the inner structure of the mitochondria. Depending on the ADP concentration, the architecture of the inner membrane can change between a condensed and an orthodox state [43]. Electron tomography revealed that in the condensed state, the matrix is compacted, and the cristae form large compartments with multiple tubular connections to the peripheral region as well as to each other. In the orthodox state, the matrix is expanded, and the cristae tend to be tubes or short flat lamellae with one or two openings in the peripheral region of the inner membrane (Fig. 3b) [82]. It has been suggested that this morphological transition could result in the elimination of diffusion bottlenecks inside large intracristal compartments that would otherwise reduce the efficiency of ATP production [82, 83].

4.2 Fusion and Fission

In healthy cells, mitochondrial fusion and fission events are in an equilibrium so that their relative rates determine the average size of the individual mitochondrial tubules and the degree of network connectivity [7, 18, 19, 56, 63, 95]. In the fission yeast *Schizosaccharomyces pombe*, the equilibrium is shifted during mitosis to fission, resulting in highly fragmented mitochondria [65]. A similar observation has been made in budding yeast cells undergoing meiosis [41]. A tempting explanation for these temporal fragmentations is the conversion of a low copy number organelle into a high copy number one, thus increasing the chance to distribute a sufficient number of mitochondria for each daughter cell to commence the next cell cycle [65, 79, 130].

Another process where excessive fission takes place is apoptosis. Upon induction of the cell death program, the mitochondrial network disintegrates, yielding numerous and smaller mitochondria (Fig. 3c) [17, 64, 137]. Whether this fragmentation of the mitochondrial network has a functional relevance for the ongoing cell death program or if it is just a by-product is still under debate [16, 38, 73, 98, 123, 137]. Apoptosis is also accompanied by a remodeling of the mitochondrial inner membrane [120, 129, 135, 136].

5 Mitochondrial Heterogeneity Within a Single Cell at a Certain Time

5.1 Morphological Heterogeneity

The distribution and shape of the mitochondria in many cultured mammalian cells are rather heterogeneous. Although they may disperse throughout the whole cytosol, frequently a pronounced tendency of aggregation around the nucleus can be observed (Figs. 1, 2a) [7, 20, 39]. But are the mitochondria of a cell luminally continuous? To address this question, Collins and coworkers performed FRAP (fluorescence recovery after photobleaching) experiments with different cell types including HeLa, PAEC, COS-7, HUVEC, cortical astrocytes and neuronal cells expressing a fluorescent protein in the mitochondrial matrix [20]. It was observed that the fluorescence in the bleached regions did not recover to >10% of its initial value 1 h after irradiation. These data suggest that in the analyzed cells, the mitochondria were largely disconnected, possibly indicating functional heterogeneities of the mitochondria within a single cell.

5.2 Functional Heterogeneity

For pancreatic acinar cells, the existence of three distinct groups of mitochondria with different functions was shown [97]: perigranular mitochondria, perinuclear

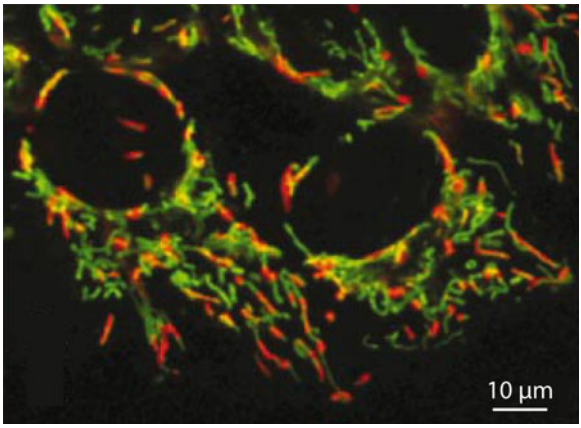

Fig. 4 Heterogeneity in the functional status of mitochondria within a single cell. Heterogeneity in the mitochondrial membrane potential is revealed by the dye JC-1 in HeLa cells. JC-1 is a green fluorescent monomer at low membrane potentials and forms orange/red fluorescent aggregates at high membrane potentials. Thus, the different colors of the fluorescence emission indicate the heterogeneity of the mitochondrial membrane potential in a single cell (from [20])

mitochondria and peripheral mitochondria near the basal plasma membrane. Photobleaching experiments indicated that these three groups are not luminally connected and respond differently to cytosolic Ca^{2+} signals. Therefore, it was suggested that they participate in the local regulation of Ca^{2+} homeostasis.

Differences between mitochondria within a single cell were not only revealed by their response to Ca^{2+} levels, but also by their membrane potential. The membrane potential is a potent functional readout of mitochondrial activity and can be monitored by using positively charged, lipophilic fluorescent dyes [62, 74, 92, 113], including JC-1 (tetrachloro-1,1,3,3-tetraethylbenzimidazol-carbocyanine-iodide) [124] and TMRM (tetramethylrhodamine-methyl-ester) [35]. JC-1 is a green fluorescent monomer at low membrane potentials and forms orange/red fluorescent aggregates at high membrane potentials. The appropriateness of JC-1 has been controversially discussed, because it provides only a qualitative readout on the membrane potential, and the staining efficiency is concentration and salt dependent [92, 126, 133]. Still, using JC-1, it was demonstrated that within a single HeLa cell, mitochondria exhibiting green fluorescence coexist with red fluorescing mitochondria (Fig. 4) [20]. Heterogeneities in the membrane potential were also conclusively reported using TMRM allowing quantitative studies [14, 28, 30, 126, 132].

These findings demonstrate that even in cells with morphologically rather similar mitochondria, pools of functionally distinct mitochondria may exist. Hence, presumably not unexpectedly, functional heterogeneities within the mitochondria were also observed in nerve cells, which exhibit a pronounced spatial and functional asymmetry. For example, in one of the largest nerve

terminals in the central nervous system of mammals, the calyx of Held [45], two mitochondrial subpopulations were described: a small mitochondrial population with complex geometries located near the presynaptic membrane called the mitochondria-associated adherens complex (MAC) and a large mitochondrial pool with a simpler architecture, which was not preferentially located near presynaptic membranes [110]. The MAC-forming mitochondria were suggested to play a central role in high rate, temporally precise neurotransmission. Further, electron tomography revealed that these MAC-forming mitochondria have a specialized ultrastructure exhibiting a polarized cristae architecture in that cristae junctions were aligned with the cytoskeleton and occurred at higher density in the mitochondrial membrane that faces the presynaptic membrane [102].

These data conclusively indicate that, at least in some cell types, morphologically and functionally distinct mitochondrial subpopulations exist. However, very little is known about whether such functional differences are due to different protein distributions within the mitochondria.

6 Nanoscopy of Protein Distributions in Mitochondria

Almost all that we know about the inner architecture of mitochondria comes from electron microscopy and electron tomography data. These techniques are very powerful for dissecting the membrane architecture of the organelles, but are generally less well suited to study the distributions of proteins, requiring specific labeling, ideally in living cells. For these challenges, fluorescence microscopy is generally the method of choice.

However, the wave nature of light imposes a seemingly fundamental limit to the attainable resolution of light microscopes. According to Abbe, the resolution limitation is ultimately rooted in the phenomenon of diffraction [1]. Because of diffraction, focusing of light always results in a blurred spot [11], whose size determines the resolution. Thus, the highest achievable resolution with objective lenses and visible light is $\sim$180 nm in the imaging plane. When using a single lens, the resolution along the optical axis is inescapably worse; even confocal or two photon fluorescence microscopes, which stand out in their ability to provide 3D images by optical sectioning, can only distinguish fluorescent objects if their axial separation is at least 500–800 nm.

For this reason, it has been impossible to resolve protein distributions within the inner membrane of unaltered mitochondria using light microscopy [134]. Likewise, the protein density in mitochondria is apparently so high that also protein complexes in the mitochondrial matrix or in the outer membrane have proved to be non-resolvable by conventional light microscopy. In fact, not very long ago, obtaining a spatial resolution sufficient to resolve inner-mitochondrial features with an optical microscope that uses lenses and focused visible light was considered unfeasible.

6.1 Concepts to Overcome the Diffraction Barrier

In recent years, a number of 'nanoscopy' or 'superresolution' fluorescence microscopy techniques have been invented to fundamentally overcome the diffraction barrier. A number of excellent and exhaustive reviews describing the theory as well as the practical details are available [47, 48, 57, 99]. Therefore, we give here only a brief overview of the concepts of the various nanoscopy schemes.

Stimulated emission depletion (STED) microscopy [53] and ground state depletion (GSD) microscopy [52] were the first concrete and viable physical concepts to fundamentally overcome the limiting role of diffraction in a lens-based optical microscope. In brief, STED and GSD use a selected pair of bright (fluorescent) and dark (non-fluorescent) fluorophore states to restrict the bright state to subdiffraction dimensions. To this end, optical transitions are utilized that allow one to transiently switch off the ability of the dye to fluoresce by confining the dye to a dark state. The transition is effected with a light intensity distribution featuring a zero, switching the fluorescence off everywhere except at the zero where the fluorophore is still allowed to be bright. Moving the zero across the specimen switches the signal of adjacent features sequentially on and off, allowing their separate registration. This allows one to image fine structures that would otherwise be blurred in a conventional diffraction-limited image. Hence, the spatial confinement of molecular states allows the elimination of the resolution-limiting effect of diffraction without eliminating the diffraction.

In its initial demonstration, STED microscopy was realized as a point-scanning system (Fig. 5), whereby the excitation focus was a normal confocal spot and the

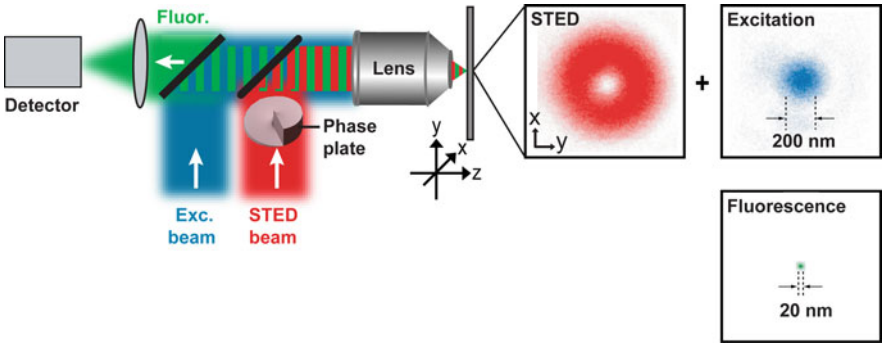

Fig. 5 Schematic drawing of a point-scanning STED microscope. Excitation and STED are accomplished with synchronized laser pulses focused by a lens onto the sample, sketched as *blue* and *red* beams, respectively. Fluorescence is registered with a detector. A phase plate is placed in the light path of the STED beam to create a ring-shaped focus featuring an intensity zero in its center. Measured intensity distributions in the focus are shown on the *right*. The diffraction limited excitation focus is overlapped with the ring-shaped STED focus. Saturated depletion confines the region of excited molecules to the zero, leaving an effective focus of subdiffraction dimensions

STED focus resembled a doughnut, featuring a light intensity zero in the center [67]. Figure 5 shows a typical experimental focal intensity distribution of the excitation spot (blue), overlapped with a STED-spot (red) featuring a central intensity zero. Saturated depletion inhibits the fluorescence everywhere except at the very center of the focal region.

Later, the concept of STED and GSD microscopy was expanded to photoswitching molecules, including synthetic organic molecules and reversibly photoswitchable fluorescent proteins (RSFPs). This family of approaches was named RESOLFT, standing for reversible saturable/switchable optical linear (fluorescence) transitions [46, 50, 51]. The RESOLFT concepts are purely "physical" or "physicochemical" concepts, because the subdiffraction resolution is a direct consequence of the molecular transition employed. Because the position of the zero is defined with the RESOLFT concepts, e.g., it is defined where the molecules are "on" and where they are "off," these concepts operate with any number of molecules, ranging from single to many (Fig. 6a).

The concept of switching is also essential in more recent far-field fluorescence nanoscopy approaches referred to here as superresolution microscopy by single-molecule switching and localization, which differ from the RESOLFT concepts by the fact that they switch molecules stochastically in space and utilize mathematics to assemble the image (Fig. 6). This family of approaches has been initially implemented independently by several groups and named photoactivated localization microscopy (PALM) [8], fluorescence photoactivated localization microscopy (FPALM) [55] and stochastic optical reconstruction microscopy (STORM) [111].

The operating principle of these concepts is to start with the vast majority of labels in an inactive (dark) state, not contributing to the fluorescence (Fig. 6b). A small fraction ($\ll 1\%$) is then stochastically transferred to the fluorescence state so that the single molecules can be individually imaged and localized to give nanometer-level precision coordinates. After the coordinates have been recorded, the bright fluorophores are then removed (e.g., by bleaching, thermal relaxation, or otherwise) so that a new subset of the fluorophores can be transferred into the fluorescent state and recorded to obtain an additional set of molecular coordinates. This process is repeated thousands of times until a sufficient number of molecular coordinates is recorded. Importantly, the molecular coordinates do not have infinite localization accuracy, but the localization accuracy depends on the number of emitted photons from the individually localized single molecule. Finally, a composite single-molecule nanoscopy image of all these coordinates is created.

6.2 Nanoscopy on Mitochondria

As described above, several studies using conventional light microscopy or electron microscopy have provided ample evidence on morphological and functional heterogeneities of mitochondria within single cells. However, due to the previous

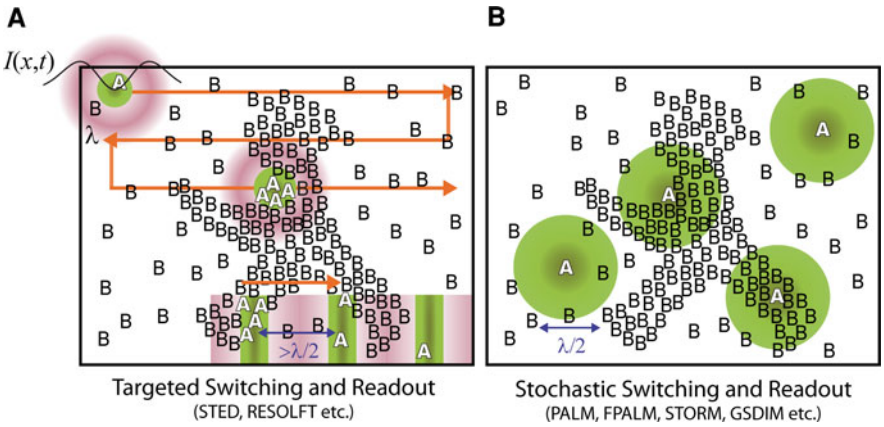

Fig. 6 Concepts to overcome the diffraction barrier. To resolve image details that are closer than the diffraction limit, all far-field fluorescence nanoscopy concepts realized so far switch the fluorophore between two distinguishable states, a bright state *A* and a dark state *B*, to construct subdiffraction images. **a** In the targeted readout mode, a spatial light intensity distribution $I(x, t)$ having a zero intensity point in space switches the molecules such that one of the states (here: *A*) is confined to subdiffraction dimensions. The image is assembled by scanning the zero over the sample and recording adjacent features sequentially in time. To parallelize the recording procedure, the zero can also be *line shaped* or an array of *zero lines*. As the zero is translated across the object, the molecules undergo several times the transition $B \rightarrow A \rightarrow B$, which explains the need for reversible transitions $A \longleftrightarrow B$. **b** The stochastic readout mode detects single fluorophores from a random position within the diffraction zone. To this end, a molecule is transferred to a state *A* that is able to emit $m \gg 1$ photons in a row, while the neighboring molecules remain in the dark state *B*. The distance between molecules in state *A* should be larger than the diffraction limit. The detection of $m \gg 1$ photons allows the calculation of the coordinate of emission from the centroid of the diffraction fluorescence spot formed on a camera. After the recording, the molecule is switched off to *B* in order to allow the recording of an adjacent molecule. If it is sufficient to record a single picture, the stochastic readout requires each molecule to cycle only once $B \rightarrow A \rightarrow B$ (adapted from [49], with permission)

lack of appropriate technologies, it is still largely unclear whether these heterogeneities also reflect heterogeneities in the sub-mitochondrial distribution of proteins. Until the advent of the nanoscopy concepts detailed above, it had proved to be very challenging or even impossible to address such questions because many mitochondrial protein complexes could not be resolved with conventional microscopy due to the limited resolution. For example, the TOM complexes, which are the primary import pores for nuclear encoded mitochondrial proteins, proved to be so densely packed in the mitochondrial outer membrane that it required STED microscopy to reveal individual TOM clusters in the mitochondrial outer membrane (Fig. 7a) [32]. Likewise, STED microscopy in combination with co-localization algorithms was used to determine quantitatively the degree of co-localization between hexokinase-I and each of the three isoforms of the human voltage-dependent anion-selective channel (hVDAC). The nanoscopy data showed

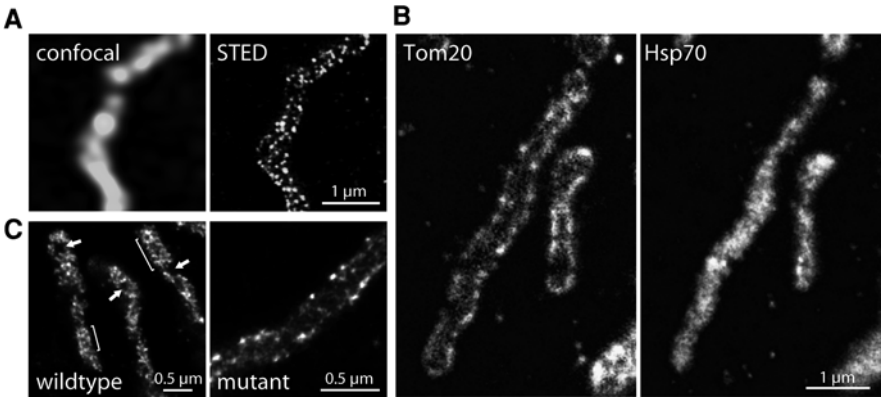

Fig. 7 STED microscopy reveals sub-mitochondrial protein distributions on the nanoscale. **a** Comparison of images taken with a (diffraction-limited) confocal microscope (*left*) and a STED microscope (*right*). The mitochondria of a PtK2 (rat kangaroo kidney) cell were labeled with an antibody against the outer membrane protein Tom20. In case of the STED image, individual Tom20 clusters are resolved, whereas they are blurred in the confocal case. **b** Two-color isoSTED images of mitochondria in Vero (African green monkey) cells allow distinguishing between proteins localized in the outer mitochondrial membrane (Tom20, *left*) and proteins of the mitochondrial matrix (Hsp70, *right*). **c** With the isoSTED approach, it is possible to reveal the arrangement of cristae, here in mammalian PtK2 cells (*left*). The cells were labeled with antibodies against the inner membrane protein complex F_1F_0ATP-synthase. The brackets indicate parallel cristae arrangements, and the arrows indicate regions devoid of cristae. Alterations in the cristae structure could be observed when depleting the protein mitofilin (*right*), which controls cristae morphology (modified from [117] and [118], with permission)

that the degree of co-localization between hVDAC and hexokinase-I is isoform-specific, suggesting a more complex interplay of these proteins than previously anticipated [91].

Recently, the implementation of STED with opposing lenses, called isoSTED microscopy, has enabled the recording of the interior of mitochondria with a 3D resolution of better than 50 nm in all room directions [117]. Using this approach, Schmidt et al. analyzed the distributions of various proteins within these organelles (Fig. 7b) [117]. By labeling the F_1F_0ATPase, a protein complex that lines the inner membrane, these authors could also delineate the flow of the inner membrane in the mitochondria of intact cells, revealing heterogeneities in the cristae arrangements (Fig. 7c) [118].

These data conclusively demonstrate that with the now widely available nanoscopy approaches, it is possible to analyze sub-mitochondrial protein distributions. We expect that in the near future these approaches will be utilized to correlate functional heterogeneities with the nanoscale distribution of mitochondrial proteins, providing new insights into the heterogeneity of mitochondria on an additional level.

7 Quantitative Image Analysis of Mitochondria

The pronounced heterogeneity of mitochondria on the functional and morphological level not only between individual cells, but also within them, immediately prohibits a biologically meaningful analysis of subtle mitochondrial differences based on individual images. A plethora of computational tools has been developed to analyze large image data sets quantitatively [4, 21–23, 30, 54, 59, 60, 69, 81, 89–91, 100, 114, 119] and have been reviewed expertly [33, 40, 44, 87, 101, 107, 121]. The availability of nanoscopy/superresolution techniques to a growing scientific community will undoubtedly further increase the need for quantitative data analysis and at the same time will elicit new challenges, including among others the fact that with these techniques the attainable optical resolution is similar to the size of the used fluorescent labels.

Acknowledgments We thank C.A. Wurm for insightful discussions and providing some of the STED images. We also thank R. Schmidt and A. Egner regarding STED microscopy of mitochondria, S.W. Hell for continuous support and J. Jethwa for carefully reading the manuscript. Part of the work reported in this review was supported by the Bundesministerium für Bildung und Forschung (BMBF) (SysCompart, to S.J.).

References

1. Abbe E (1873) Beiträge zur Theorie des Mikroskops und der mikroskopischen Wahrnehmung. Arch f Mikroskop Anat 9:413–420
2. Amchenkova AA, Bakeeva LE, Chentsov YS et al (1988) Coupling membranes as energy-transmitting cables. I. Filamentous mitochondria in fibroblasts and mitochondrial clusters in cardiomyocytes. J Cell Biol 107:481–495
3. Arimura S, Tsutsumi N (2002) A dynamin-like protein (ADL2b), rather than FtsZ, is involved in *Arabidopsis* mitochondrial division. Proc Natl Acad Sci USA 99:5727–5731
4. Barbe L, Lundberg E, Oksvold P et al (2008) Toward a confocal subcellular atlas of the human proteome. Mol Cell Proteomics 7:499–508
5. Benard G, Bellance N, James D et al (2007) Mitochondrial bioenergetics and structural network organization. J Cell Sci 120:838–848
6. Benda C (1898) Ueber dier Spermatogenese de Verbebraten und höherer Evertebraten, II. Theil: Die Histogenese der Spermien. Arch Anat Physiol 73:393–398
7. Bereiter-Hahn J (1990) Behavior of mitochondria in the living cell. Int Rev Cytol 122:1–63
8. Betzig E, Patterson GH, Sougrat R et al (2006) Imaging intracellular fluorescent proteins at nanometer resolution. Science 313:1642–1645
9. Bodenstein-Lang J, Buch A, Follmann H (1989) Animal and plant mitochondria contain specific thioredoxins. FEBS Lett 258:22–26
10. Bogorad L (2008) Evolution of early eukaryotic cells: genomes, proteomes, and compartments. Photosynth Res 95:11–21
11. Born M, Wolf E (2002) Principles of optics. Cambridge University Press, Cambridge
12. Brandon M, Baldi P, Wallace DC (2006) Mitochondrial mutations in cancer. Oncogene 25:4647–4662
13. Brocard JB, Rintoul GL, Reynolds IJ (2003) New perspectives on mitochondrial morphology in cell function. Biol Cell 95:239–242

14. Buckman JF, Reynolds IJ (2001) Spontaneous changes in mitochondrial membrane potential in cultured neurons. J Neurosci 21:5054–5065
15. Carew JS, Huang P (2002) Mitochondrial defects in cancer. Mol Cancer 1:9
16. Cassidy-Stone A, Chipuk JE, Ingerman E et al (2008) Chemical inhibition of the mitochondrial division dynamin reveals its role in Bax/Bak-dependent mitochondrial outer membrane permeabilization. Dev Cell 14:193–204
17. Cereghetti GM, Scorrano L (2006) The many shapes of mitochondrial death. Oncogene 25:4717–4724
18. Cerveny KL, Tamura Y, Zhang Z et al (2007) Regulation of mitochondrial fusion and division. Trends Cell Biol 17:563–569
19. Chan DC (2006) Mitochondrial fusion and fission in mammals. Annu Rev Cell Dev Biol 22:79–99
20. Collins TJ, Berridge MJ, Lipp P et al (2002) Mitochondria are morphologically and functionally heterogeneous within cells. EMBO J 21:1616–1627
21. Comeau JW, Costantino S, Wiseman PW (2006) A guide to accurate fluorescence microscopy colocalization measurements. Biophys J 91:4611–4622
22. Conrad C, Gerlich DW (2010) Automated microscopy for high-content RNAi screening. J Cell Biol 188:453–461
23. Costes SV, Daelemans D, Cho EH et al (2004) Automatic and quantitative measurement of protein-protein colocalization in live cells. Biophys J 86:3993–4003
24. Crabtree HG (1929) Observations on the carbohydrate metabolism of tumours. Biochem J 23:536–545
25. Danial NN, Korsmeyer SJ (2004) Cell death: critical control points. Cell 116:205–219
26. De Deken RH (1966) The Crabtree effect: a regulatory system in yeast. J Gen Microbiol 44:149–156
27. Detmer SA, Chan DC (2007) Functions and dysfunctions of mitochondrial dynamics. Nat Rev Mol Cell Biol 8:870–879
28. Diaz G, Falchi AM, Gremo F et al (2000) Homogeneous longitudinal profiles and synchronous fluctuations of mitochondrial transmembrane potential. FEBS Lett 475:218–224
29. Diaz-Ruiz R, Averet N, Araiza D et al (2008) Mitochondrial oxidative phosphorylation is regulated by fructose 1,6-bisphosphate. A possible role in Crabtree effect induction? J Biol Chem 283:26948–26955
30. Distelmaier F, Koopman WJ, Testa ER et al (2008) Life cell quantification of mitochondrial membrane potential at the single organelle level. Cytometry A 73:129–138
31. Dlaskova A, Spacek T, Santorova J et al (2010) 4Pi microscopy reveals an impaired three-dimensional mitochondrial network of pancreatic islet beta-cells, an experimental model of type-2 diabetes. Biochim Biophys Acta 1797:1327–1341
32. Donnert G, Keller J, Wurm CA et al (2007) Two-color far-field fluorescence nanoscopy. Biophys J 92:L67–69
33. Dragunow M (2008) High-content analysis in neuroscience. Nat Rev Neurosci 9:779–788
34. Egner A, Jakobs S, Hell SW (2002) Fast 100-nm resolution three-dimensional microscope reveals structural plasticity of mitochondria in live yeast. Proc Natl Acad Sci USA 99: 3370–3375
35. Ehrenberg B, Montana V, Wei MD et al (1988) Membrane potential can be determined in individual cells from the nernstian distribution of cationic dyes. Biophys J 53:785–794
36. Fernandez-Moreno MA, Bornstein B, Petit N et al (2000) The pathophysiology of mitochondrial biogenesis: towards four decades of mitochondrial DNA research. Mol Genet Metab 71:481–495
37. Fiechter A, Fuhrmann GF, Kappeli O (1981) Regulation of glucose metabolism in growing yeast cells. Adv Microb Physiol 22:123–183
38. Frank S, Gaume B, Bergmann-Leitner ES et al (2001) The role of dynamin-related protein 1, a mediator of mitochondrial fission, in apoptosis. Dev Cell 1:515–525
39. Frazier AE, Kiu C, Stojanovski D et al (2006) Mitochondrial morphology and distribution in mammalian cells. Biol Chem 387:1551–1558

40. Glory E, Murphy RF (2007) Automated subcellular location determination and high-throughput microscopy. Dev Cell 12:7–16
41. Gorsich SW, Shaw JM (2004) Importance of mitochondrial dynamics during meiosis and sporulation. Mol Biol Cell 15:4369–4381
42. Green DR, Kroemer G (2004) The pathophysiology of mitochondrial cell death. Science 305:626–629
43. Hackenbrock CR (1966) Ultrastructural bases for metabolically linked mechanical activity in mitochondria. I. Reversible ultrastructural changes with change in metabolic steady state in isolated liver mitochondria. J Cell Biol 30:269–297
44. Hamilton N (2009) Quantification and its applications in fluorescent microscopy imaging. Traffic 10:951–961
45. Held H (1893) Die centrale Gehorleitung. Arch f Anat u Physiol Anat Abt 201–248
46. Hell SW (2003) Toward fluorescence nanoscopy. Nat Biotechnol 21:1347–1355
47. Hell SW (2007) Far-field optical nanoscopy. Science 316:1153–1158
48. Hell SW (2009a) Far-field optical nanoscopy. In: Single molecule spectroscopy in chemistry, physics and biology. Springer, Berlin
49. Hell SW (2009b) Microscopy and its focal switch. Nat Methods 6:24–32
50. Hell SW, Dyba M, Jakobs S (2004) Concepts for nanoscale resolution in fluorescence microscopy. Curr Opin Neurobiol 14:599–609
51. Hell SW, Jakobs S, Kastrup L (2003) Imaging and writing at the nanoscale with focused visible light through saturable optical transitions. Appl Phys A (Materials Science Processing) 77:859–860
52. Hell SW, Kroug M (1995) Ground-state depletion fluorescence microscopy, a concept for breaking the diffraction resolution limit. Appl Phys B 60:495–497
53. Hell SW, Wichmann J (1994) Breaking the diffraction resolution limit by stimulated emission: stimulated emission depletion microscopy. Opt Lett 19:780–782
54. Herold J, Schubert W, Nattkemper TW (2010) Automated detection and quantification of fluorescently labeled synapses in murine brain tissue sections for high throughput applications. J Biotechnol. doi:10.1016/j.jbiotec.2010.03.004
55. Hess ST, Girirajan TP, Mason MD (2006) Ultra-high resolution imaging by fluorescence photoactivation localization microscopy. Biophys J 91:4258–4272
56. Hoppins S, Lackner L, Nunnari J (2007) The machines that divide and fuse mitochondria. Annu Rev Biochem 76:751–780
57. Huang B, Bates M, Zhuang X (2009) Super-resolution fluorescence microscopy. Annu Rev Biochem 78:993–1016
58. Huang HM, Fowler C, Zhang H et al (2004) Mitochondrial heterogeneity within and between different cell types. Neurochem Res 29:651–658
59. Huh WK, Falvo JV, Gerke LC et al (2003) Global analysis of protein localization in budding yeast. Nature 425:686–691
60. Hutchins JR, Toyoda Y, Hegemann B et al (2010) Systematic analysis of human protein complexes identifies chromosome segregation proteins. Science 328:593–599
61. Jacobson J, Duchen MR (2004) Interplay between mitochondria and cellular calcium signalling. Mol Cell Biochem 256–257:209–218
62. Jakobs S (2006) High resolution imaging of live mitochondria. Biochim Biophys Acta 1763:561–575
63. Jakobs S, Martini N, Schauss AC et al (2003) Spatial and temporal dynamics of budding yeast mitochondria lacking the division component Fis1p. J Cell Sci 116:2005–2014
64. Jourdain A, Martinou JC (2009) Mitochondrial outer-membrane permeabilization and remodelling in apoptosis. Int J Biochem Cell Biol 41:1884–1889
65. Jourdain I, Gachet Y, Hyams JS (2009) The dynamin related protein Dnm1 fragments mitochondria in a microtubule-dependent manner during the fission yeast cell cycle. Cell Motil Cytoskeleton 66:509–523
66. Kennedy EP, Lehninger AL (1949) Oxidation of fatty acids and tricarboxylic acid cycle intermediates by isolated rat liver mitochondria. J Biol Chem 179:957–972

67. Klar TA, Jakobs S, Dyba M et al (2000) Fluorescence microscopy with diffraction resolution barrier broken by stimulated emission. Proc Natl Acad Sci USA 97:8206–8210
68. Kölliker A (1857) Einige Bemerkungen über die Endigungen der Hautnerven und den Bau der Muskeln. Zeitschr f wissensch Zool 8:311–325
69. Koopman WJ, Visch HJ, Smeitink JA et al (2006) Simultaneous quantitative measurement and automated analysis of mitochondrial morphology, mass, potential, and motility in living human skin fibroblasts. Cytometry A 69:1–12
70. Kroemer G (2003) Mitochondrial control of apoptosis: an introduction. Biochem Biophys Res Commun 304:433–435
71. Kuznetsov AV, Hermann M, Saks V et al (2009) The cell-type specificity of mitochondrial dynamics. Int J Biochem Cell Biol 41:1928–1939
72. Kwong JQ, Beal MF, Manfredi G (2006) The role of mitochondria in inherited neurodegenerative diseases. J Neurochem 97:1659–1675
73. Lee YJ, Jeong SY, Karbowski M et al (2004) Roles of the mammalian mitochondrial fission and fusion mediators Fis1, Drp1, and Opa1 in apoptosis. Mol Biol Cell 15:5001–5011
74. Lemasters JJ, Ramshesh VK (2007) Imaging of mitochondrial polarization and depolarization with cationic fluorophores. Methods Cell Biol 80:283–295
75. Liesa M, Palacin M, Zorzano A (2009) Mitochondrial dynamics in mammalian health and disease. Physiol Rev 89:799–845
76. Lill R (2009) Function and biogenesis of iron-sulphur proteins. Nature 460:831–838
77. Logan DC (2006) Plant mitochondrial dynamics. Biochim Biophys Acta 1763:430–441
78. Logan DC, Leaver CJ (2000) Mitochondria-targeted GFP highlights the heterogeneity of mitochondrial shape, size and movement within living plant cells. J Exp Bot 51:865–871
79. Lowe M, Barr FA (2007) Inheritance and biogenesis of organelles in the secretory pathway. Nat Rev Mol Cell Biol 8:429–439
80. Mackenzie S, McIntosh L (1999) Higher plant mitochondria. Plant Cell 11:571–586
81. Manders E, Verbeek FJ, Aten JA (1993) Measurement of co-localization of objects in dual-colour confocal images. J Micros 169:375–382
82. Mannella CA (2006) Structure and dynamics of the mitochondrial inner membrane cristae. Biochim Biophys Acta 1763:542–548
83. Mannella CA, Pfeiffer DR, Bradshaw PC et al (2001) Topology of the mitochondrial inner membrane: dynamics and bioenergetic implications. IUBMB Life 52:93–100
84. McBride HM, Neuspiel M, Wasiak S (2006) Mitochondria: more than just a powerhouse. Curr Biol 16:R551–560
85. Meisinger C, Sickmann A, Pfanner N (2008) The mitochondrial proteome: from inventory to function. Cell 134:22–24
86. Modica-Napolitano JS, Kulawiec M, Singh KK (2007) Mitochondria and human cancer. Curr Mol Med 7:121–131
87. Muzzey D, van Oudenaarden A (2009) Quantitative time-lapse fluorescence microscopy in single cells. Annu Rev Cell Dev Biol 25:301–327
88. Navarro A, Boveris A (2007) The mitochondrial energy transduction system and the aging process. Am J Physiol Cell Physiol 292:C670–686
89. Negishi T, Nogami S, Ohya Y (2009) Multidimensional quantification of subcellular morphology of *Saccharomyces cerevisiae* using CalMorph, the high-throughput image-processing program. J Biotechnol 141:109–117
90. Neumann B, Walter T, Heriche JK et al (2010a) Phenotypic profiling of the human genome by time-lapse microscopy reveals cell division genes. Nature 464:721–727
91. Neumann D, Bückers J, Kastrup L et al (2010b) Two-color STED microscopy reveals different degrees of colocalization between hexokinase-I and the three human VDAC isoforms. PMC Biophys 3:4
92. Nicholls DG, Ward MW (2000) Mitochondrial membrane potential and neuronal glutamate excitotoxicity: mortality and millivolts. Trends Neurosci 23:166–174
93. Nishikawa T, Araki E (2007) Impact of mitochondrial ROS production in the pathogenesis of diabetes mellitus and its complications. Antioxid Redox Signal 9:343–353

94. Nishino I, Kobayashi O, Goto Y et al (1998) A new congenital muscular dystrophy with mitochondrial structural abnormalities. Muscle Nerve 21:40–47
95. Nunnari J, Marshall WF, Straight A et al (1997) Mitochondrial transmission during mating in *Saccharomyces cerevisiae* is determined by mitochondrial fusion and fission and the intramitochondrial segregation of mitochondrial DNA. Mol Biol Cell 8:1233–1242
96. Okamoto K, Shaw JM (2005) Mitochondrial morphology and dynamics in yeast and multicellular eukaryotes. Annu Rev Genet 39:503–536
97. Park MK, Ashby MC, Erdemli G et al (2001) Perinuclear, perigranular and sub-plasmalemmal mitochondria have distinct functions in the regulation of cellular calcium transport. EMBO J 20:1863–1874
98. Parone PA, James DI, Da Cruz S et al (2006) Inhibiting the mitochondrial fission machinery does not prevent Bax/Bak-dependent apoptosis. Mol Cell Biol 26:7397–7408
99. Patterson G, Davidson M, Manley S et al (2010) Superresolution Imaging using Single-Molecule Localization. Annu Rev Phys Chem 61:346–367
100. Peng T, Bonamy GM, Glory-Afshar E et al (2010) Determining the distribution of probes between different subcellular locations through automated unmixing of subcellular patterns. Proc Natl Acad Sci USA 107:2944–2949
101. Pepperkok R, Ellenberg J (2006) High-throughput fluorescence microscopy for systems biology. Nat Rev Mol Cell Biol 7:690–696
102. Perkins GA, Tjong J, Brown JM et al (2010) The micro-architecture of mitochondria at active zones: electron tomography reveals novel anchoring scaffolds and cristae structured for high-rate metabolism. J Neurosci 30:1015–1026
103. Premsler T, Zahedi RP, Lewandrowski U et al (2009) Recent advances in yeast organelle and membrane proteomics. Proteomics 9:4731–4743
104. Rasmusson AG, Geisler DA, Moller IM (2008) The multiplicity of dehydrogenases in the electron transport chain of plant mitochondria. Mitochondrion 8:47–60
105. Rebeille F, Alban C, Bourguignon J et al (2007) The role of plant mitochondria in the biosynthesis of coenzymes. Photosynth Res 92:149–162
106. Reddy PH (2009) Amyloid beta, mitochondrial structural and functional dynamics in Alzheimer's disease. Exp Neurol 218:286–292
107. Rittscher J (2010) Characterization of biological processes through automated image analysis. Annu Rev Biomed Eng 12:315–344
108. Rizzuto R, Pinton P, Carrington W et al (1998) Close contacts with the endoplasmic reticulum as determinants of mitochondrial Ca^{2+} responses. Science 280:1763–1766
109. Rossignol R, Gilkerson R, Aggeler R et al (2004) Energy substrate modulates mitochondrial structure and oxidative capacity in cancer cells. Cancer Res 64:985–993
110. Rowland KC, Irby NK, Spirou GA (2000) Specialized synapse-associated structures within the calyx of Held. J Neurosci 20:9135–9144
111. Rust M, Bates M, Zhuang X (2006) Sub-diffraction-limit imaging by stochastic optical reconstruction microscopy (STORM). Nat Methods 3:793–795
112. Saraste M (1999) Oxidative phosphorylation at the fin de siecle. Science 283:1488–1493
113. Scaduto RC Jr, Grotyohann LW (1999) Measurement of mitochondrial membrane potential using fluorescent rhodamine derivatives. Biophys J 76:469–477
114. Schauss AC, Bewersdorf J, Jakobs S (2006) Fis1p and Caf4p, but not Mdv1p, determine the polar localization of Dnm1p clusters on the mitochondrial surface. J Cell Sci 119:3098–3106
115. Scheffler IE (2001) Mitochondria make a come back. Adv Drug Deliv Rev 49:3–26
116. Scheffler IE (2008) Mitochondria. Wieley, New Jersey
117. Schmidt R, Wurm CA, Jakobs S et al (2008) Spherical nanosized focal spot unravels the interior of cells. Nat Methods 5:539–544
118. Schmidt R, Wurm CA, Punge A et al (2009) Mitochondrial cristae revealed with focused light. Nano Lett 9:2508–2510

119. Schubert W, Bonnekoh B, Pommer AJ et al (2006) Analyzing proteome topology and function by automated multidimensional fluorescence microscopy. Nat Biotechnol 24:1270–1278
120. Scorrano L, Ashiya M, Buttle K et al (2002) A distinct pathway remodels mitochondrial cristae and mobilizes cytochrome *c* during apoptosis. Dev Cell 2:55–67
121. Shariff A, Kangas J, Coelho LP et al (2010) Automated image analysis for high-content screening and analysis. J Biomol Screen. doi:10.1177/1087057110370894
122. Sheahan MB, McCurdy DW, Rose RJ (2005) Mitochondria as a connected population: ensuring continuity of the mitochondrial genome during plant cell dedifferentiation through massive mitochondrial fusion. Plant J 44:744–755
123. Sheridan C, Delivani P, Cullen SP et al (2008) Bax- or Bak-induced mitochondrial fission can be uncoupled from cytochrome *c* release. Mol Cell 31:570–585
124. Smiley ST, Reers M, Mottola-Hartshorn C et al (1991) Intracellular heterogeneity in mitochondrial membrane potentials revealed by a J-aggregate-forming lipophilic cation JC-1. Proc Natl Acad Sci USA 88:3671–3675
125. Stevens B (1977) Variation in number and volume of the mitochondria in yeast according to growth conditions. A study based on serial sectioning and computer graphics reconstitution. Biol Cell 28:37–56
126. Sträuber H, Müller S (2010) Viability states of bacteria-specific mechanisms of selected probes. Cytometry A. doi:10.1002/cyto.a.20920
127. Szabadkai G, Simoni AM, Bianchi K et al (2006) Mitochondrial dynamics and Ca^{2+} signaling. Biochim Biophys Acta 1763:442–449
128. Thomas B, Beal MF (2007) Parkinson's disease. Hum Mol Genet 16(2):R183–194
129. Wang C, Youle RJ (2009) The role of mitochondria in apoptosis. Annu Rev Genet 43:95–118
130. Warren G, Wickner W (1996) Organelle inheritance. Cell 84:395–400
131. Weber K, Ridderskamp D, Alfert M et al (2002) Cultivation in glucose-deprived medium stimulates mitochondrial biogenesis and oxidative metabolism in HepG2 hepatoma cells. Biol Chem 383:283–290
132. Wikstrom JD, Katzman SM, Mohamed H et al (2007) beta-Cell mitochondria exhibit membrane potential heterogeneity that can be altered by stimulatory or toxic fuel levels. Diabetes 56:2569–2578
133. Wikstrom JD, Twig G, Shirihai OS (2009) What can mitochondrial heterogeneity tell us about mitochondrial dynamics and autophagy? Int J Biochem Cell Biol 41:1914–1927
134. Wurm CA, Jakobs S (2006) Differential protein distributions define two subcompartments of the mitochondrial inner membrane in yeast. FEBS Lett 580:5628–5634
135. Yamaguchi R, Lartigue L, Perkins G et al (2008) Opa1-mediated cristae opening is Bax/Bak and BH3 dependent, required for apoptosis, and independent of Bak oligomerization. Mol Cell 31:557–569
136. Yamaguchi R, Perkins G (2009) Dynamics of mitochondrial structure during apoptosis and the enigma of Opa1. Biochim Biophys Acta 1787:963–972
137. Youle RJ, Karbowski M (2005) Mitochondrial fission in apoptosis. Nat Rev Mol Cell Biol 6:657–663
138. Zellnig G, Zechmann B, Perktold A (2004) Morphological and quantitative data of plastids and mitochondria within drought-stressed spinach leaves. Protoplasma 223:221–227